

## pH-profile crystal structure studies of C-terminal despentapeptide nitrite reductase from *Achromobacter cycloclastes*

Hai-Tao Li,<sup>a</sup> Chao Wang,<sup>a</sup> Tschining Chang,<sup>b</sup> Wen-Chang Chang,<sup>b,c</sup> Ming-Yih Liu,<sup>d</sup> Jean Le Gall,<sup>d</sup> Lu-lu Gui,<sup>a</sup> Ji-Ping Zhang,<sup>a</sup> Xiao-Min An,<sup>a</sup> and Wen-Rui Chang<sup>a,\*</sup>

<sup>a</sup> National Laboratory of Biomacromolecules, Institute of Biophysics, Chinese Academy of Sciences, 15th Datun Road, Chaoyang District, Beijing 100101, China

<sup>b</sup> Institute of Biological Chemistry, Academia Sinica, Taipei 11529, Taiwan

<sup>c</sup> Institute of Biochemical Sciences, National Taiwan University, Taipei 106, Taiwan

<sup>d</sup> Department of Biochemistry and Molecular Biology, University of Georgia, Athens, GA 30602-7229, USA

Received 15 January 2004

This work is dedicated to Prof. Jean Le Gall (1932–2003).

### Abstract

Crystal structures of C-terminal despentapeptide nitrite reductase (NiRc-5) from *Achromobacter cycloclastes* were determined from 1.9 to 2.3 Å at pH 5.0, 5.4, and 6.2. NiRc-5, that has lost about 30% activity, is found to possess quite similar trimeric structures as the native enzyme. Electron density and copper content measurements indicate that the activity loss is not caused by the release of type 2 copper (T2Cu). pH-profile structural comparisons with native enzyme reveal that the T2Cu active center in NiRc-5 is perturbed, accounting for the partial loss of enzyme activity. This perturbation likely results from the less constrained conformations of two catalytic residues, Asp98 and His255. Hydrogen bonding analysis shows that the deletion of five residues causes a loss of more than half the intersubunit hydrogen bonds mediated by C-terminal tail. This study shows that the C-terminal tail plays an important role in controlling the conformations around the T2Cu site at the subunit interface, and helps keep the optimum microenvironment of active center for the full enzyme activity of AcNiR.

© 2004 Elsevier Inc. All rights reserved.

**Keywords:** Crystal structure; Denitrification; Nitrite reductase; Residue deletion; pH profile; *Achromobacter cycloclastes*

Dissimilatory nitrite reductases (NiRs) catalyze the reduction of nitrite to nitric oxide, the first step in the denitrification pathway to produce a gaseous product, and result in the direct loss of fixed nitrogen from the terrestrial environment [1]. Two classes of NiRs, the heme cd1 and the copper NiRs (CuNiR), have been identified so far; they are entirely different in their three-dimensional structures. NiR isolated from *Achromobacter cycloclastes* (AcNiR) belongs to the copper type and is the first CuNiR whose crystal structure has been determined [2,3]. Structure studies show that CuNiR is a homo-trimer with each monomer comprising two Greek key  $\beta$ -barrel domains. A total of six copper atoms are

found in the trimer and could be classified into two types. The type 1 copper (T1Cu) is buried within the N-terminal domain of each monomer and is coordinated by the residues His95, Cys136, His145, and Met150, serving as the chromophoric center and the site of electron transfer in CuNiR. The type 2 copper (T2Cu) is located at the subunit interface and is ligated by one water and three histidine residues (His100, His135, and His306), serving as the site for nitrite binding and reduction. The two copper sites are approximately 12.5 Å apart and are closely linked through sequence segments 135–136 and 95–100, which form a well-engineered T1Cu–T2Cu configuration that is of high efficiency for both intramolecular electron transfer and nitrite reduction [4–6]. Two water-bridged residues in the vicinity of T2Cu, Asp98 and His255, are catalytically critical residues.

\* Corresponding author. Fax: +86-10-6488-9867.

E-mail address: [wchang@sun5.ibp.ac.cn](mailto:wchang@sun5.ibp.ac.cn) (W.-R. Chang).

Previous studies showed that they are involved not only in the catalytic reaction but also in the substrate anchoring and the intramolecular electron transfer [7–9].

The AcNiR trimer is very stable in that it can resist the dissociation of SDS at room temperature even when the concentration is as high as 4% (w/v) (unpublished data). Crystal structure studies reveal an unusual but conserved elongated C-terminal tail in CuNiR. It extends from one monomer to another, forming hydrogen bond interactions between monomers, and has been considered as one of the key factors for maintaining the trimeric structure of CuNiR [2]. We have generated a series of C-terminally deleted AcNiR mutants to study the role of C-terminal tail in AcNiR. Interestingly, it was shown that the C-terminal segment is essential for maintaining the enzyme activity as well as the quaternary structure of AcNiR [10]. Despentapeptide nitrite reductase (NiRc-5) is the AcNiR analogue with five residues (336–340) deleted from C-terminus. NiRc-5 still maintains as rigid trimer, showing typical native enzyme optical spectrum, but has lost about 30% activity. It is the first C-terminally shortened AcNiR mutant that begins to lose part of the enzyme activity [10]. Adman et al. [3] have reported the crystal structure studies of AcNiR at five different pH values, providing detailed comparisons and descriptions of AcNiR structures. To perform a systematic comparison with native enzyme and detect changes that occurred to NiRc-5 after the residue deletion, we report here a similar pH profile (pH 5.0, 5.4, and 6.2) crystal structure study of NiRc-5.

## Materials and methods

**Protein crystallization.** The NiRc-5 was crystallized as described earlier [11]. Using a similar precipitant solution containing ammonium sulfate, orthorhombic crystals were obtained by the hanging drop method under three different pH values: 5.0, 5.4, and 6.2. The pH of the crystals was taken as the nominal pH of the buffers used for crystallization. The pH 5.0 and 5.4 solutions were buffered by acetate

acid, and the pH 6.2 solution was buffered by Mes. For clarity, data and coordinate sets from crystals at pH 5.0, 5.4, and 6.2 are designated NC50, NC54, and NC62.

**Data collection and processing.** Data collection and processing of NC62 and NC50 crystals have been described previously [11]; the data were collected at 100 K and were finally processed to 1.9 and 2.2 Å, respectively. The NC54 data set was collected at room temperature on beam line BL6B at Photon Factory (Tsukuba, Japan) using a Weissenberg camera. The data were processed to 2.29 Å using programs DENZO and SCALEPACK [12]. NC54 crystal also belongs to  $P2_12_12_1$  space group with cell parameters:  $a = 101.5$  Å,  $b = 118.2$  Å, and  $c = 124.7$  Å. The overall  $R$ -merge, completeness, and signal-to-noise ratio ( $I/\sigma$ ) of NC54 data within 20–2.29 Å are 12.7%, 97.4%, and 11.0%, respectively. The cell volume of NC54 crystal is slightly larger than those of NC62 and NC50, which should be a result of the different data-collecting temperature [11].

**Structure determination.** The structure of NC54 was solved by molecular replacement method using the program Amore [13]. As there was a trimer in the asymmetric unit [11], the structure of AcNiR trimer (PDBid: 1NIA) was chosen as starting model after deleting all solvent and copper atoms and the C-terminal five residues, and yielded a distinct solution with correlation coefficient of 0.82 and  $R$ -factor of 26.9% in 20–3 Å. The structure was then refined by program CNS [14] using the maximum likelihood methods to a  $R$ -factor of 15.5%. Using the refined NC54 structure as starting model, NC62 was solved by molecular replacement method similar to NC54 and was refined to a  $R$ -factor of 17.9% by CNS. As NC50 and NC62 crystals are same in crystal form, the initial phase of NC50 was obtained with the isomorphous difference Fourier method using the NC62 model and was then refined to a  $R$ -factor of 18.1% by CNS. During the refinements of all structures, no constraints were applied to the coordination geometry of copper; a threefold non-crystallographic symmetry (NCS) restraint was used in earlier stages of refinement and was totally released at last. All model buildings and adjustments were carried out manually using the O program [15] on an SGI workstation. Stereochemistry of refined model was monitored by program PROCHECK [16] and no residues were found in the disallowed region of the Ramachandran plot in all models. Refinement statistics of all structures are summarized in Table 1. The coordinate files and structure factors of NC62 and NC50 have been deposited into Protein Data Bank with reference numbers 1RZP and 1RZQ, respectively.

**Copper content measurement.** To verify the crystallographic results relating to the loss of T2Cu, the copper content of NiRc-5 was also measured. Copper concentration was determined with the plasma emission spectrophotometer. The protein concentration was determined using the Lowry method [17].

Table 1  
Refinement statistics of NiRc-5 structures

	NC62	NC54	NC50
Structure			
Resolution (Å)	20–1.9	20–2.29	20–2.2
Reflections used ( $F > 0\sigma F$ )	107,773	63,040	69,668
Completeness (%)	95.1	92.7	95.2
Working $R$ -factor (%)	17.9	15.5	18.1
Free $R$ -factor (%)	19.1	17.9	20.8
r.m.s.d. bonds (Å)	0.005	0.005	0.005
r.m.s.d. angles (°)	1.6	1.5	1.6
Number of residues/waters	988/835	988/513	988/796
Average $B$ -factor			
Main chain (Å <sup>2</sup> )	17.7	24.3	21.4
Side chain (Å <sup>2</sup> )	19.8	27.3	23.1
Water (Å <sup>2</sup> )	27.6	36.9	29.8
Ramachandran plot (non-Gly, non-Pro)			
Most favored region	89.0%	89.1%	87.8%
Additionally allowed region	11.0%	10.9%	12.2%

## Results and discussion

### Overall structure

The refined models of all three NiRc-5 structures comprise 988 residues and six copper atoms in the asymmetric unit. The residues that have been modeled consist of A8–A335, B8–B335, and C4–C335. No electron density was observed for the N-terminal seven residues of chains A and B, which are similar to native enzyme; while the residues 4–7 of chain C appear in the electron density map as they participate in crystal packing and were built into the model. The remaining tail residues in NiRc-5 structures fit the electron density very well except the last residue Val335, which bears a high *B*-factor and dispersed electron density (Fig. 1A). Compared with native AcNiR, the overall structure of NiRc-5 is not affected by the deletion of the five residues. NiRc-5 still exists as a homo-trimer (Fig. 1B) and all secondary structural elements in native structure are well retained. The  $C\alpha$  superimposition of NC54 trimer with AcNiR (PDBid: 1NIA) yielded only a RMS deviation of 0.24 Å.

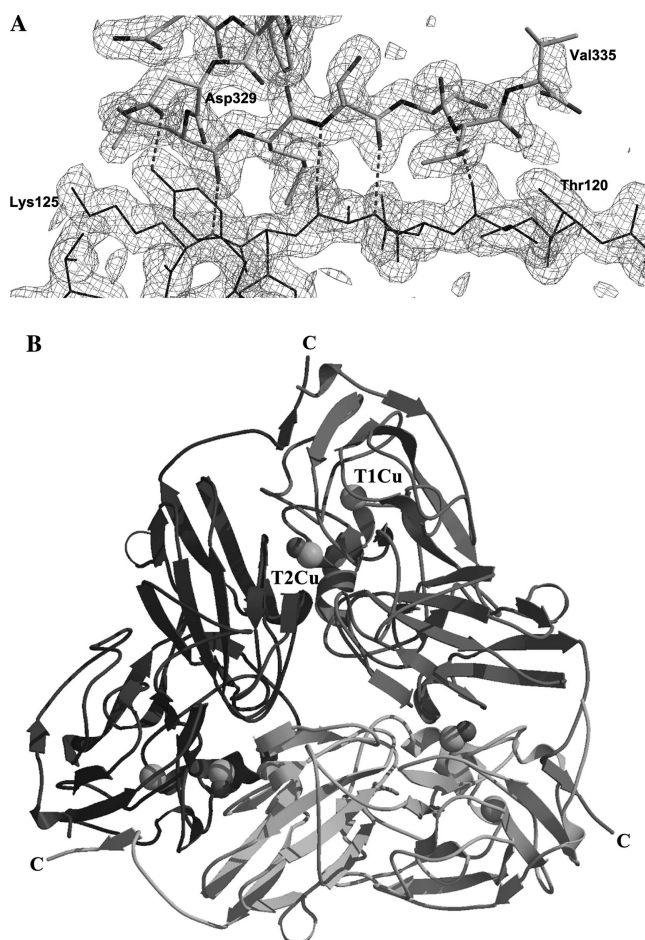


Fig. 1. (A)  $2F_o - F_c$  electron density map ( $1.0 \sigma$ ) around the C-terminal tail. (B) NiRc-5 trimer. All figures in this paper are produced using programs Molscript [22] and Raster3D [23].

Except for Val335, which moves outwards, the remaining C-terminal segment (324–334) is almost in the same configuration as AcNiR and also forms an anti-parallel  $\beta$ -sheet with strand 121–125 of the adjacent subunit (Fig. 1A). No systematic differences, other than a few reorientations of the side chains, are found between the NiRc-5 structures under different pH values. The  $C\alpha$ -based superimposition of NC62 with NC50 gives a RMS deviation of 0.17 Å, which shows that the NiRc-5 trimer is still a well-constructed object resistant to change with pH as AcNiR [3].

### Copper sites configuration

As shown in Fig. 2, superimposition of the copper sites in NiRc-5 with native protein shows no significant difference in the configuration of the two copper centers, except that residues 96–98 of the linking stretch His95–His100 shift slightly towards the T2Cu. Inspection of the copper coordination statistics also revealed that there is little difference in copper site geometry between NiRc-5 and AcNiR. Most of the changes in Cu–ligand distance and Cu–ligand bond angle are within 0.1 Å and  $5^\circ$ , respectively. In view that the copper sites are the chromophoric and catalytic centers [4], the similarities to the native enzyme in both arrangement and coordination geometry of the two copper sites are consistent with the unchanged optical spectrum and retained more than two-thirds specific activity of NiRc-5.

### Enzyme activity loss and the T2Cu occupancy

T2Cu is located at the cleft formed by two adjacent monomers and tends to lose from the protein in enzyme preparation or other drastic conditions. Libby and Averill [18] have shown that the specific activity of Cu-NiR is directly proportional to the occupancy of T2Cu. In the pH-profile crystal structure study of AcNiR [3], Adman et al. found that the most significant difference occurs in the occupancy of T2Cu at the active site. Since the release of T2Cu from AcNiR is prone to take place, and the specific activity is closely related to the occupancy of T2Cu, the lowered activity of NiRc-5 might be a result of the partial loss of T2Cu. However, electron density at the T2Cu site indicates that the loss of T2Cu does not occur. In all three structures of NiRc-5, the T2Cu displays stronger electron density than T1Cu at nearly all  $\sigma$  levels, indicating that the occupancy of T2Cu is no less than that of T1Cu. As the T1Cu buried in each monomer is normally fully occupied, most likely the T2Cu of NiRc-5 is in full occupancy. To ensure this crystallographic result, copper content was measured by plasma emission spectroscopy and was found to be  $\sim 6.0$  of coppers per NiRc-5 trimer. These results clearly show that the lowered activity of NiRc-5 was not caused by the partial loss of T2Cu; there should be other subtle

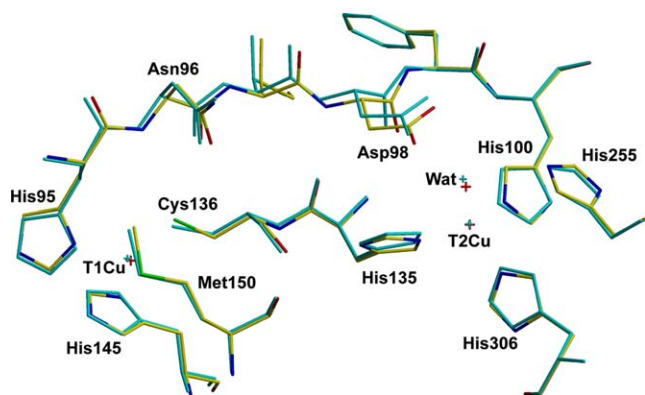


Fig. 2. Superimposition of NiRc-5 (mixed color) and AcNiR (cyan) around the copper sites. The whole configuration around the copper sites of NiRc-5 and AcNiR is quite similar except for the slight shift of residues 96–98 towards T2Cu in NiRc-5. Superimposition is performed in program O [15] and based on the C $\alpha$  of the whole trimer. The superimposed chain A of NC62 and 1N1A (AcNiR) [3] are taken as example and shown here; superimposition of other chains and structures gives similar results, including the slight shift of residues 96–98.

structural changes accounting for the activity loss of NiRc-5.

#### pH-profile structural comparison with AcNiR

Although the partial loss of T2Cu did not take place, a pH-profile structural comparison with AcNiR revealed that the microenvironment around T2Cu site was perturbed in NiRc-5.

(a)  $F_o - F_o$  difference map around T2Cu. In the previous structure study of AcNiR by Adman et al. [3],  $F_o - F_o$  difference maps were calculated between data sets of the same crystal form, and displayed clear difference electron density at T2Cu site and side chain of Asp98, reflecting the variable occupancies of T2Cu and the different thermal parameters of Asp98. Fig. 3A illustrates the  $F_o - F_o$  difference map around T2Cu site between NC62 and NC50. Apparently, no significant difference in electron density could be seen at both T2Cu site and side chain of Asp98. In contrast, considerable difference in electron density appears around the T2Cu ligand water and the imidazole ring of His255. Such differences show that the occupancy of T2Cu is no more susceptible to the pH change in NiRc-5.

(b)  $B$ -factor statistics around copper sites. Selected  $B$ -factor statistics around the two copper sites are listed in Table 2. In all three NiRc-5 structures, the  $B$ -factors of T2Cu are considerably lower than those of T1Cu, revealing a more ordered T2Cu. On the contrary, all T2Cu in AcNiR structures exhibit higher or comparable  $B$ -factors to T1Cu; especially in the structure at pH 5.0, similar  $B$ -factor is obtained only when the occupancy of T2Cu is set to 0.8 [3]. The difference in  $B$ -factors between T1Cu and T2Cu in NiRc-5 shows a

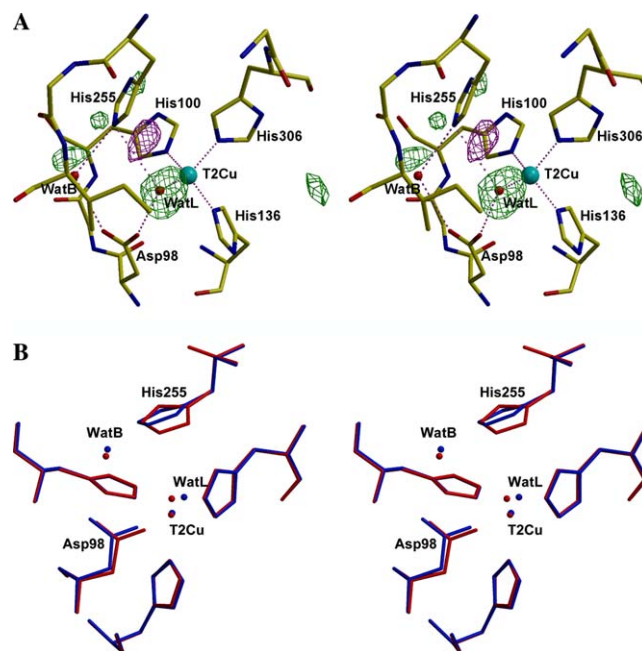


Fig. 3. (A) NC50–NC62  $F_o - F_o$  difference maps around T2Cu site. Positive maps (green) and negative maps (magenta) are contoured at 6.0  $\sigma$  level. The large positive map around the ligand water (WatL) suggests a more ordered WatL in NC50. The positive and negative maps flanking His255 side chain suggest the rotation of the imidazole ring. No significant difference map appears around the T2Cu. The represented model is the averaged pdb file of NC50 and NC62, which is used to supply the phase information for  $F_o - F_o$  difference map calculation by program CNS [14]. (B) The superimposed structure around T2Cu site in NC62 (red) and NC50 (blue). Catalytic residues His255 and Asp98 are related by a bridging water (WatB) and a ligand water (WatL); they undergo cooperative conformational changes when pH rises from 5.0 to 6.2. Rotation of His255 side chain towards WatL in NC62 is clear. Superimposition is performed in program O [15] and based on the C $\alpha$  of the whole trimer. Changes are similar in all three superimposed chains and only chain A is displayed here.

well-encapsulated T2Cu, consistent with the represented electron density. An unexpected finding from Table 2 is that the T2Cu ligand water exhibits a regular increase of  $B$ -factor following the rise of pH. At pH 5.0, the  $B$ -factor of WatL is significantly lower than that of T2Cu (about one-half lower) in NiRc-5; at pH 5.4, it is about one-quarter higher; while at pH 6.2, the WatL  $B$ -factor becomes about one half higher. In contrast, the  $B$ -factors of WatL in all AcNiR structures are consistently lower than those of T2Cu and no obvious increase of  $B$ -factor can be detected even when the pH rises to 6.8 [3]. The NC50–NC62 difference map (Fig. 3A) also displays clear positive electron density around WatL, corresponding to a well-bound WatL in NC50 and a less ordered WatL in NC62. Since the optimum pH of AcNiR activity is 6.2 [19] and nitrite displaces the ligand water during the reaction [3,20], the increased  $B$ -factor of WatL in NC62 structure indicates that the effective nitrite binding might be disturbed in NiRc-5.

Table 2  
Selected *B*-factors (Å<sup>2</sup>) around the copper site of NiRc-5 and AcNiR

ID	NC50	NC54	NC62	1NIE <sup>a</sup>	2NRD <sup>a</sup>	1NIA <sup>a</sup>
T1Cu	27.2 (0.2) <sup>b</sup>	27.5 (1.4)	21.2 (1.8)	19.0	18.8	8.4 (3.1)
T2Cu	20.0 (0.8)	17.9 (1.7)	15.3 (1.2)	19.0 [ <i>Q</i> = 0.8] <sup>c</sup>	18.1	11.7 (0.9)
WatL	10.9 (0.6)	22.4 (2.4)	23.0 (1.6)	16.7	17.6	9.3 (0.4)
WatB	16.1 (5.3)	20.3 (2.0)	18.4 (2.2)	15.5	17.7	17.0 (4.9)
Asp98	23.7 (1.1)	21.1 (2.1)	17.4 (2.6)	20.8	20.4	11.6 (0.2)
His255	15.2 (1.0)	18.2 (2.6)	13.5 (0.9)	10.9	16.6	4.3 (0.9)

<sup>a</sup> 1NIE, 2NRD, and 1NIA are the PDB entry code of AcNiR structures under pH 5.0, 5.4, and 6.2, respectively [3].

<sup>b</sup> Values in parentheses are the average deviation of the three chains.

<sup>c</sup> The occupancy (*Q*) of T2Cu was set to 0.8 so as to meet a similar *B*-factor behavior as T1Cu.

(c) *pH*-dependent conformational change of His255 side chain. Comparison between NiRc-5 structures shows that the side chain of His255 bears a pH-dependent conformational change after the residue deletion. At higher pH conditions, residue His255 in NC54 and NC62 adopts a similar side chain conformation, in which the N<sup>ε2</sup> atom of imidazole ring lies approaching WatL, while when the pH drops to 5.0, the imidazole ring of His255 rotates about 25° and departs from WatL (Fig. 3B). The rotation of the His255 side chain is also suggested in the NC50–NC62 difference map, where positive and negative electron densities appear at each side of the His255 imidazole ring (Fig. 3A). In contrast, no obvious conformational changes of the His255 side chain could be observed among the AcNiR structures at five pH values [3]. The His255 side chain in AcNiR adopts a similar conformation as in NiRc-5 at higher pH.

From the differences around the T2Cu site between NiRc-5 and AcNiR in response to pH change, it can be inferred that the microenvironment around T2Cu including the copper ligand water and two catalytic residues (Asp98 and His255) is affected by the deletion of five residues. Because the T2Cu is the active center where nitrite binding and reduction take place, such changes probably disturb the effective nitrite binding and affect the cooperativity of the catalytic residues in nitrite reduction, therefore leading to the partial activity loss of NiRc-5.

#### Catalytic residues and perturbation of T2Cu Site

Catalytic residues Asp98 and His255, being close but not ligating to T2Cu, are from two adjacent monomers

and could be related by a bridging water (WatB) and a ligand water (WatL) as illustrated in Fig. 3B. Distance statistics listed in Table 3 show that at pH 5.4 and 6.2, the H255N<sup>ε2</sup>–WatL distances in NiRc-5 decrease from ~3.78 Å (NC50) to ~3.01 Å (NC54) and ~3.16 Å (NC62), suggesting formation of hydrogen bonds at higher pH. In addition, the rotation of His255 side chain towards WatL in NC54 and NC62 also supports a hydrogen bonding attraction between H255N<sup>ε2</sup> and WatL, whereas no such hydrogen bond could be deduced in NC50 as judged from both distance and conformation (Table 3 and Fig. 3B). The incapability of forming a hydrogen bond between His255 and WatL at pH 5.0 most likely results from the largely protonated His255 side chain as WatL, which can only act as proton donor after ligating to T2Cu, needs a proton acceptor to complete hydrogen bonding. The atomic structure of CuNiR from *Alcaligenes xylosoxidans* (PDBid: 1OE1) [21] recently determined at pH 6.5 reveals a H255N<sup>ε2</sup>–WatL distance of 2.92 Å, also showing the existence of hydrogen bond interaction between H255 side chain and WatL at higher pH; while the crystal structure of CuNiR from *Alcaligenes faecalis* (PDBid: 1AS7) [20] determined at pH 4.5 shows almost the same His255 side chain conformation as that in NC50 and gives a H255N<sup>ε2</sup>–WatL distance of ~4.00 Å, consistent with the loss of hydrogen bond between H255N<sup>ε2</sup> and WatL at low pH.

Asp98 and His255 are located at the opposite sides of WatL and both are capable of forming hydrogen bond with WatL at higher pH. Obviously, there exists a hydrogen-bonded competition for WatL between the two catalytic residues as each has the tendency of drawing

Table 3  
Distance between catalytic residues and neighboring water

ID (Å)	NC50	NC54	NC62	1NIE <sup>a</sup>	2NRD <sup>a</sup>	1NIA <sup>a</sup>
Resolution	2.2	2.29	1.9	1.9	2.1	2.5
D98O <sup>δ1</sup> –WatL	2.73 (0.02) <sup>b</sup>	2.51 (0.05)	2.50 (0.06)	2.39	2.79	2.78 (0.07)
H255N <sup>ε2</sup> –WatL	3.78 (0.02)	3.01 (0.03)	3.16 (0.06)	3.63	3.41	3.13 (0.13)
D98O <sup>δ2</sup> –WatB	3.34 (0.03)	2.94 (0.04)	3.04 (0.06)	3.05	2.98	3.03 (0.16)
H255N <sup>ε2</sup> –WatB	2.89 (0.06)	3.37 (0.02)	3.13 (0.05)	3.30	3.32	3.20 (0.15)

<sup>a</sup> 1NIE, 2NRD, and 1NIA are the PDB entry code of AcNiR structures under pH 5.0, 5.4, and 6.2, respectively [3].

<sup>b</sup> Values in parentheses are the average deviation of the three chains in an asymmetric crystallographic unit.

the WatL closer so as to fit its own optimum hydrogen bonding geometry. As shown in Table 3, the distances of both H255N<sup>e2</sup>–WatL and D98O<sup>δ1</sup>–WatL in NiRc-5 become shorter when the pH changes from 5.0 to 6.2, indicating both hydrogen bonds are strengthened. We propose that at pH 6.2, the competition has become so strong that a scramble for WatL occurs in NiRc-5, which is likely to bring about the positional disorder of WatL and therefore results in the increased *B*-factor and dispersed electron density of WatL in NC62.

Although no significant conformational change of the His255 side chain could be detected in AcNiR, the distance of H255N<sup>e2</sup>–WatL also contracts from 3.63 Å (pH 5.0) via 3.41 Å (pH 5.4) to ~3.13 Å (pH 6.2) when the pH increases (Table 3), indicating a similar hydrogen bond between H255N<sup>e2</sup> and WatL is formed at pH 6.2. However, differing from NiRc-5, the D98O<sup>δ1</sup>–WatL distance in AcNiR stretches from 2.39 to ~2.78 Å when the pH changes from 5.0 to 6.2, showing weakened hydrogen bonding between D98O<sup>δ1</sup> and WatL in AcNiR at pH 6.2 (Table 3). It should also be noted that the D98O<sup>δ1</sup>–WatL hydrogen bond length in AcNiR at higher pH (5.4 and 6.2) is about 0.3 Å longer than in NiRc-5 at similar pH (Table 3). The weakened D98O<sup>δ1</sup>–WatL hydrogen bonding in combination with the unchanged *B*-factor of WatL in various AcNiR structures strongly suggests that the scramble for WatL by Asp98 and His255 does not exist in AcNiR at pH 6.2. Superimposition at T2Cu site with AcNiR reveals a slight main chain movement of residues 96–98 towards T2Cu in NiRc-5 (Fig. 2), in which the C $\alpha$  of Asp98 displays a displacement of ~0.4 Å, a key feature that should account for the perturbation of WatL in NiRc-5. The approach of Asp98 towards T2Cu and the pH-depend

ent rotation of His255 side chain in NiRc-5 suggests that the conformations of both catalytic residues are less constrained after the deletion of the five residues from C-terminus.

#### *Pentapeptide deletion and enzyme activity loss*

NiRc-5 is the first C-terminally deleted AcNiR analogue that begins to lose part of the enzyme activity [10]. As listed in Table 4, the number of intersubunit hydrogen bonds mediated by the C-terminal tail reduces from 11 to 5 after the pentapeptide deletion. The loss of more than half the hydrogen bonds in NiRc-5 should be significant and likely have impaired the function of the C-terminal tail in maintaining the enzyme activity. Val335 forms three intersubunit hydrogen bonds in AcNiR but fails to retain either of them due to its conformational change in NiRc-5 (Fig. 1A), which is a major factor in the significant loss of hydrogen bonds. Conformational change of Val335 in NiRc-5 might be consequent on the deletion of Lys336. In native AcNiR structure, residue Lys336 forms a water-bridged hydrogen bond between monomers [3] and probably plays a role in protecting Val335 against the perturbations from solvent.

#### *Role of C-terminal tail in maintaining the activity of AcNiR*

Crystallographic studies on AcNiR have shown that the C-terminal tail forms an anti-parallel  $\beta$ -sheet with strand 117–125 of another monomer and helps to maintain a stable CuNiR trimer; the tail is also spatially adjacent to sequence segment 103–115, which constitutes the

Table 4  
Intersubunit hydrogen bonds mediated by C-terminal tail in NiRc-5 and AcNiR

AcNiR (1NIA, Chain C) <sup>a</sup>					
1	C329	Asp OD1	B80	Tyr OH	2.35 Å
2	C330	Leu O	B125	Lys N	3.20 Å
3	C332	Thr O	B123	Arg N	2.99 Å
4	C332	Thr N	B123	Arg O	2.91 Å
5	C334	Val O	B121	Thr O	2.72 Å
6	C335	Val O	B120	Thr OG1	2.59 Å
7	C335	Val O	B121	Thr N	2.94 Å
8	C335	Val N	B121	Thr O	3.02 Å
9	C338	Ala O	B119	Glu N	3.03 Å
10	C338	Ala N	B119	Glu O	3.10 Å
11	C340	Met N	B117	Gly O	2.83 Å
NiRc-5 (NC62, Chain C) <sup>b</sup>					
1	C329	Asp OD1	B80	Tyr OH	2.53 Å
2	C330	Leu O	B125	Lys N	2.80 Å
3	C332	Thr O	B123	Arg N	2.99 Å
4	C332	Thr N	B123	Arg O	2.86 Å
5	C334	Val N	B121	Thr O	2.89 Å

<sup>a</sup> 1NIA is the PDB entry code of AcNiR structure at pH 6.2 [3].

<sup>b</sup> It is similar in other chains and structures at different pH.

side wall for the active pocket, and thus indirectly participates the maintenance of the T2Cu active center [3]. These crystallographic studies show that the local environments at the T2Cu site are perturbed in NiRc-5 and such perturbation most likely results from the less constrained conformations of two catalytic residues after the deletion of five residues. Based on the above discussions, we propose that the C-terminal tail, though not directly participating in the active center formation, plays an important role in controlling the conformations around the T2Cu site at the subunit interface, and helps to keep the optimum microenvironment of active center for the full enzyme activity of AcNiR.

### Acknowledgments

We thank Prof. N. Sakabe and Dr. K. Sakabe in the Photon Factory (Tsukuba, Japan) for the help in data collection. The project was supported by the National Key Research Development of China (Project No. G1999075601), National Key Special Research Program (2002BA711A12), and Knowledge Innovation Program of Chinese Academy of Sciences (KJCS2-SW-N06).

### References

- [1] W.G. Zumft, Cell biology and molecular basis of denitrification, *Microbiol. Mol. Biol. Rev.* 61 (1997) 533–616.
- [2] J.W. Godden, S. Turley, D.C. Teller, E.T. Adman, M.Y. Liu, W.J. Payne, J. LeGall, The 2.3 angstrom X-ray structure of nitrite reductase from *Achromobacter cycloclastes*, *Science* 253 (1991) 438–442.
- [3] E.T. Adman, J.W. Godden, S. Turley, The structure of copper-nitrite reductase from *Achromobacter cycloclastes* at five pH values, with NO<sub>2</sub><sup>-</sup> bound and with type II copper depleted, *J. Biol. Chem.* 270 (1995) 27458–27474.
- [4] S. Suzuki, K. Kataoka, K. Yamaguchi, T. Inoue, Y. Kai, Structure–function relationships of copper-containing nitrite reductases, *Coord. Chem. Rev.* 190–192 (1999) 245–265.
- [5] F.E. Dodd, J. Van Beeumen, R.R. Eady, S.S. Hasnain, X-ray structure of a blue-copper nitrite reductase in two crystal forms. The nature of the copper sites, mode of substrate binding and recognition by redox partner, *J. Mol. Biol.* 282 (1998) 369–382.
- [6] R.W. Strange, L.M. Murphy, F.E. Dodd, Z.H. Abraham, R.R. Eady, B.E. Smith, S.S. Hasnain, Structural and kinetic evidence for an ordered mechanism of copper nitrite reductase, *J. Mol. Biol.* 287 (1999) 1001–1009.
- [7] K. Kataoka, H. Furusawa, K. Takagi, K. Yamaguchi, S. Suzuki, Functional analysis of conserved aspartate and histidine residues located around the type 2 copper site of copper-containing nitrite reductase, *J. Biochem. (Tokyo)* 127 (2000) 345–350.
- [8] M.J. Boulanger, M. Kukimoto, M. Nishiyama, S. Horinouchi, M.E. Murphy, Catalytic roles for two water bridged residues (Asp-98 and His-255) in the active site of copper-containing nitrite reductase, *J. Biol. Chem.* 275 (2000) 23957–23964.
- [9] M.J. Boulanger, M.E. Murphy, Alternate substrate binding modes to two mutant (D98N and H255N) forms of nitrite reductase from *Alcaligenes faecalis* S-6: structural model of a transient catalytic intermediate, *Biochemistry* 40 (2001) 9132–9141.
- [10] W.C. Chang, J.Y. Chen, T. Chang, M.Y. Liu, W.J. Payne, J. LeGall, W.C. Chang, The C-terminal segment is essential for maintaining the quaternary structure and enzyme activity of the nitric oxide forming nitrite reductase from *Achromobacter cycloclastes*, *Biochem. Biophys. Res. Commun.* 250 (1998) 782–785.
- [11] H.T. Li, T. Chang, M.Y. Liu, J. LeGall, X.M. An, L.L. Gui, J.P. Zhang, D.C. Liang, W.R. Chang, Preliminary crystallographic studies of two C-terminally truncated copper-containing nitrite reductases from *Achromobacter cycloclastes*: changed crystallizing behaviors caused by residue deletion, *Biochem. Biophys. Res. Commun.* 299 (2002) 173–176.
- [12] Z. Otwinowski, W. Minor, Processing of X-ray diffraction data collected in oscillation mode, *Methods Enzymol.* 276 (1996) 307–326.
- [13] J. Navaza, Amore: an automated package for molecular replacement, *Acta Crystallogr. A* 50 (1994) 157–163.
- [14] A.T. Brunger, P.D. Adams, G.M. Clore, W.L. DeLano, P. Gros, R.W. Grosse-Kunstleve, J.S. Jiang, J. Kuszewski, M. Nilges, N.S. Pannu, R.J. Read, L.M. Rice, T. Simonson, G.L. Warren, Crystallography & NMR system: a new software suite for macromolecular structure determination, *Acta Crystallogr. D Biol. Crystallogr.* 54 (1998) 905–921.
- [15] T.A. Jones, J.Y. Zou, S.W. Cowan, Kjelsgaard, Improved methods for building protein models in electron density maps and the location of errors in these models, *Acta Crystallogr. A* 47 (1991) 110–119.
- [16] R.A. Laskowski, M.W. MacArthur, D.S. Moss, J.M. Thornton, PROCHECK: a program to check the stereochemical quality of protein structures, *J. Appl. Crystallogr.* 26 (1993) 283–291.
- [17] O.H. Lowry, N.J. Rosebrough, A.L. Farr, R.J. Randall, Protein measurement with the folin phenol reagent, *J. Biol. Chem.* 193 (1951) 265–275.
- [18] E. Libby, B.A. Averill, Evidence that the type 2 copper centers are the site of nitrite reduction by *Achromobacter cycloclastes* nitrite reductase, *Biochem. Biophys. Res. Commun.* 187 (1992) 1529–1535.
- [19] H. Iwasaki, S. Noji, S. Shidara, *Achromobacter cycloclastes* nitrite reductase. The function of copper, amino acid composition, and ESR spectra, *J. Biochem. (Tokyo)* 78 (1975) 355–361.
- [20] M.E. Murphy, S. Turley, E.T. Adman, Structure of nitrite bound to copper-containing nitrite reductase from *Alcaligenes faecalis*, *J. Biol. Chem.* 272 (1997) 28455–28460.
- [21] M.J. Ellis, F.E. Dodd, G. Sawers, R.R. Eady, S.S. Hasnain, Atomic resolution structures of native copper nitrite reductase from *Alcaligenes xylosoxidans* and the active site mutant Asp92Glu, *J. Mol. Biol.* 328 (2003) 429–438.
- [22] P.J. Kraulis, MOLSCRIPT: a program to produce both detailed and schematic plots of protein structures, *J. Appl. Crystallogr.* 24 (1991) 946–950.
- [23] E.A. Merritt, D.J. Bacon, Raster3D: photorealistic molecular graphics, *Methods Enzymol.* 277 (1997) 505–524.